Downloaded from UvA-DARE, the institutional repository of the University of Amsterdam (UvA)
http://dare.uva.nl/document/154280

File ID	154280
Filename	Chapter 6: Discussion : controlled light exposure microscopy implementations in fluorescence live-cell microscopy to reduce phototoxicity and photobleaching

SOURCE (OR PART OF THE FOLLOWING SOURCE):

Type	Dissertation
Title	Controlled light exposure microscopy
Author	R.A. Hoebe
Faculty	Faculty of Medicine
Year	2010
Pages	127

FULL BIBLIOGRAPHIC DETAILS:
http://dare.uva.nl/record/322972

Copyright

It is not permitted to download or to forward/distribute the text or part of it without the consent of the author(s) and/or copyright holder(s), other then for strictly personal, individual use.

UvA-DARE is a service provided by the library of the University of Amsterdam (http://dare.uva.nl)

Chapter 6

Discussion:

Controlled light exposure microscopy implementations in fluorescence live-cell microscopy to reduce phototoxicity and photobleaching

Controlled light exposure microscopy implementations in fluorescence live-cell microscopy to reduce phototoxicity and photobleaching

Ron A. Hoebe

Centre for Microscopy Research (CMO), Department of Cell Biology and Histology, Academic Medical Centre, Amsterdam, The Netherlands

Abstract

Controlled light exposure microscopy (CLEM) is a recently developed technology designed for reduction of phototoxicity and photobleaching in fluorescence (live-cell) microscopy. Fluorescence live-cell imaging is always a trade-off between image quality and damage induced by excitation light to the cells that are imaged. CLEM reduces phototoxicity and photobleaching in cells under investigation by limiting excitation of fluorophores in parts of the field of view that do not need high image quality. CLEM has been implemented successfully in standard single-point confocal microscopy reducing phototoxicity and photobleaching 2- to 10-fold. Here, we discuss the prospects of implementation of CLEM in other fluorescence live-cell microscopy techniques.

CLEM

CLEM is a new technology that has been developed to reduce phototoxicity and photobleaching in fluorescence live-cell imaging [1-3]. In live-cell microscopy, a compromise has to be found between, on the one hand, collection of data that provides a high enough signal-to-noise ratio (S/N) to enable quantitative measurements of a living specimen and, on the other hand, prevention of cell damage and bleaching [4;5]. Because phototoxicity and photobleaching is predominantly caused by excitation of fluorophores [6-11], the intensity of excitation light in fluorescence microscopy is usually tuned to the lowest level that allows detection of weak foreground signals with acceptable S/N [12-14]. Consequently, in bright foreground, where the fluorescence signal is relatively high, the S/N is higher than necessary for good image quality (Fig 1A). Therefore, CLEM reduces illumination of bright foreground areas without affecting image quality (Fig. 1B). Similarly, in background areas between fluorescent objects, illumination does not contribute to image quality (Fig. 1A). Again, CLEM reduces illumination in the background without affecting image quality (Fig. 1B). In short, CLEM prevents unnecessary excitation of fluorophores in live-cell microscopy not needed for image quality by spatially controlling the excitation light dose.

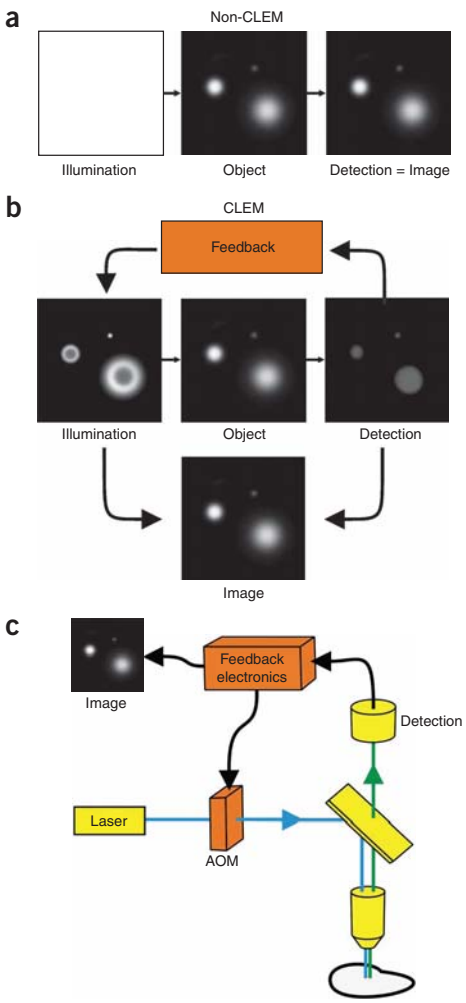

Figure 1 The concept and implementation of CLEM. (**A**) Non-CLEM imaging is based on uniform illumination of a field of view. A detector directly captures the image of the field of view and, consequently, gives direct information on the objects. Illumination light for excitation of the fluorescent objects in non-CLEM is not used optimally and leads to unnecessary phototoxicity and photobleaching. (**B**) CLEM is based on non-uniform illumination of the field of view. Light for the excitation of fluorophores is spatially controlled and used only where it is necessary for good image quality. The excitation light dose represented by the illumination image is reduced in fluorophore-dense regions (bright foreground) and in the background between objects. The image of the objects is estimated by extrapolation on the basis of the illumination light dose and the detection signal for each pixel. (**C**) A fast electronic feedback system controls illumination by operation of an acoustic-optical modulator (AOM) depending on signals from the emission light detector and calculates the signal reflecting the fluorophore concentration to form an image. This figure is reproduced from Nature Biotechnology Ref. 1 © (2007) Macmillan Publishers Ltd.

CLEM implementation in a scanning confocal microscope

In a standard scanning confocal microscope, imaging is performed pixel by pixel by scanning a laser beam across the field of view. A pinhole prevents out-of-focus light to reach the detector. Fluorescence detection in a single pixel of the image is linearly depending on the light exposure dose in this single pixel.

Implementation of CLEM in a scanning confocal microscope [15] required two alterations of the setup. An acoustic-optical modulator (AOM) is placed in the laser beam to switch the illumination light on and off within the pixel dwell time. A fast electronic feedback system controls the AOM pixel by pixel depending on signals from the emission light detector and estimates by linear extrapolation the signal reflecting the fluorophore concentration in each pixel to form an image (Fig 1C). In this way, CLEM reduces photobleaching and phototoxicity 2- to 10-fold.

The effect of CLEM on phototoxicity is shown in Fig. 2A where a series of images was captured in time of live HeLa cells expressing the H2B-GFP fusion protein with non-CLEM and CLEM, respectively. Cells imaged with non-CLEM showed blebbing of cell membranes after approximately 30 min. After approximately 3 hours, most cells were rounded-up and apoptotic. In CLEM, blebbing occurred after approximately 3 hours

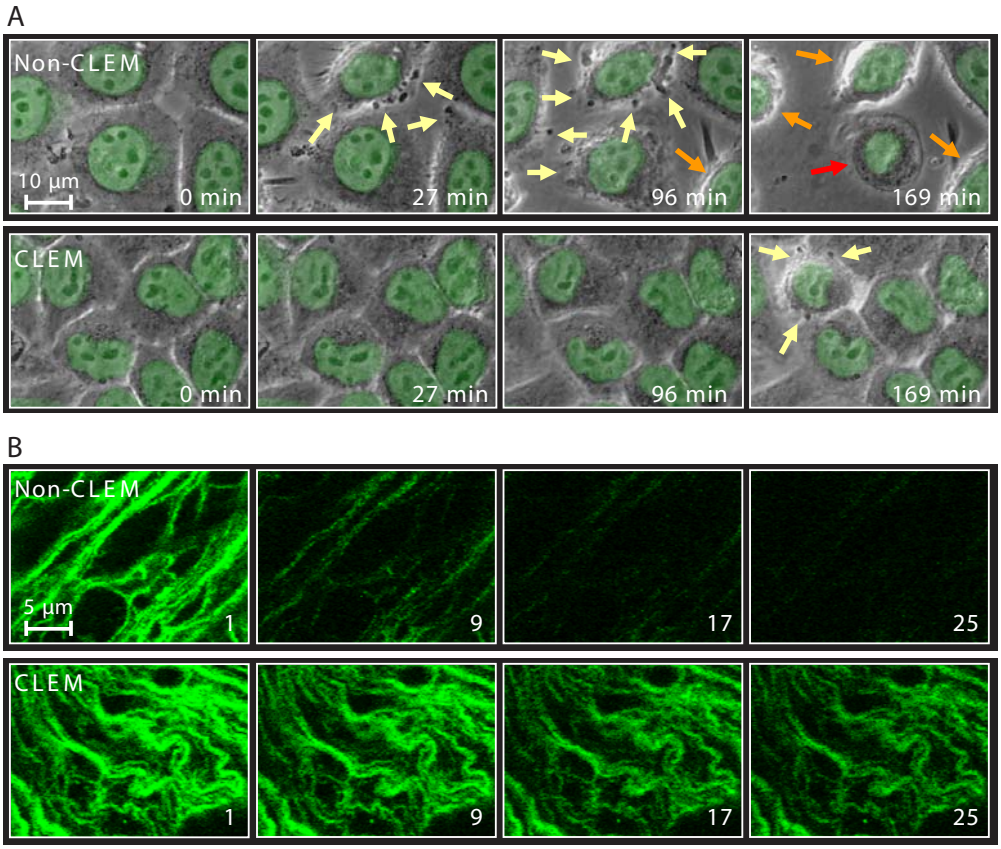

Figure 2 CLEM reduces phototoxicity and photobleaching. (**A**) Series of 3D images of living H2B-GFP-expressing HeLa cells in time in which the GFP signal is superimposed on the phase-contrast images. Cells illuminated with non-CLEM show blebbing of the membrane (yellow arrows) after 27 minutes of exposure. After 96 minutes, some cells begin to round-up (orange arrows) and after 169 minutes some cells are apoptotic (red arrow). By applying CLEM, this process is delayed by a factor of 6. (**B**) The difference in photobleaching characteristics between non-CLEM and CLEM is clearly visible in series of 3D stacks of tobacco BY-2 cells expressing microtubules-associated GFP-MAP4. Analysis of photobleaching curves shows that the bleach rate is 7-fold reduced by CLEM. This figure is reproduced from Nature Biotechnology Ref. 1 © (2007) Macmillan Publishers Ltd.

only. Apparently, reduction of the excitation light dose by CLEM allows prolonged live-cell imaging (here, approx. 6 times longer) without loss of image quality. The effect of CLEM on photobleaching is shown in Fig. 2B where a series of single optical sections from 3D images was captured in time with non-CLEM and CLEM, respectively, of fixed tobacco plant BY-2 cells expressing a microtubule reporter MAP4 fused with GFP. Bleaching curves showed that the bleach rate in CLEM was 7-fold slower than the bleach rate in non-CLEM.

The CLEM factor, a quantitative measure of reduction in phototoxicity and photobleaching

Reduction of phototoxicity and photobleaching depends on the fluorophore distribution in the sample, the optical properties

of the confocal microscope and settings of the CLEM electronic feedback system. Simulations showed that especially the fluorophore distribution and the reduction of illumination in the background determines the extent of reduction of phototoxicity and photobleaching reduction. The CLEM factor takes these parameters into account and serves as a quantitative measure of reduction in phototoxicity and photobleaching in CLEM [16].

Noise in CLEM

To prevent phototoxicity and photobleaching as much as possible during imaging of living cells by confocal microscopy, the excitation light dose is reduced as much as possible irrespective of CLEM being used or not. Therefore, live cell imaging has to deal with low signals and consequently with a low S/N (typically between 5 and 10). In confocal microscopy, noise is generally caused by the stochastic character of light [13].This stochastic character of light has a consequence for image formation in CLEM. Especially the reduction of illumination in the background in CLEM can generate artefacts in the CLEM image. These artefacts are visible as erratic "darker pixels" in the foreground with a lower pixel value than the neighboring pixels. In CLEM, the decision whether a pixel belongs to the background or foreground is performed in a preset fraction of the full pixel exposure time. There is a probability that, due to photon noise, a pixel is judged to be background despite the fact that the pixel belongs to the foreground. Linear extrapolation of the value of this pixel leads to an incorrect (too low) estimation of the value after full exposure ("darker pixels"). A special adaptive image processing filter can detect these "darker pixels" and calculates a better estimation of the pixel value which substitutes the too low value [17] (Fig. 3 A,C,E).

An alternative method to prevent "darker pixels" is predictive CLEM [3]. In predictive CLEM, values of already measured pixels are used to calculate light exposure for an upcoming pixel. Illumination can be switched off as fast as possible or the illumination can be tuned down during the full pixel exposure time. Both illumination schemes do not lead to "darker pixels" in the foreground. A possible incorrect applied illumination dose leads only to more or less noise and not to extrapolation errors. In addition, the predictive CLEM background decision is less sensitive to photon noise because the decisions are based on photons collected in more than one pixel. Therefore, the advantage of predictive CLEM is the fact that values of already measured neighbouring pixels (in space and/or time) provide, than when the signal in one pixel is monitored, a better estimate of the fluorescence in the pixel to be measured. This is correct only when (spatial and temporal) pixel sampling is at Nyquist rate [12;13]. Otherwise, the values of neighbouring pixels deviate too much from each other and the fluorescence in the pixel to be measured cannot be properly estimated. The simulation in Fig. 3 shows the performance of predictive CLEM, but implementation of predictive CLEM in a confocal microscope is needed to show its real value in practice.

Reduction of the illumination power during the full exposure time in a pixel consequently decreases the photon rate in this pixel. This allows for the application of

more sensitive detectors (for example an avalanche photodiode (APD)) that have a limited dynamic range. The most important consequence is further reduction of phototoxicity and photobleaching. In theory, the predictive CLEM factor can reach values of up to 100 depending on the fluorophore distribution and dynamics of objects in the sample. It seems that predictive CLEM is the best choice in case of imaging at the Nyquist rate in a standard scanning confocal microscope. In the case of scanning below the Nyquist rate, CLEM based on the signal in the measured pixel only is a good alternative when combined with the special adaptive filter for removal of "darker pixels".

CLEM in a biological context

Recently, CLEM was applied in a biological context [18]. Mammalian cells with fluorescently-labeled telomeres (ECV-304 cells stably expressing TRF1 and TRF2-mCitrine) were imaged for over 24 hours without significant photodamage as cells proliferation was not hampered. Fig. 4 illustrates the beneficial effect of CLEM showing the reduction of photobleaching without loss of image quality. CLEM combined with fluorescence after photobleaching (FRAP) and fluorescence loss in photobleaching (FLIP) showed that telomeres dynamically associate in small territories and TRF1 and TRF2 are abundantly present in these territories but not firmly bound. A long-term CLEM experiment showed that the bulk of TRF protein dissociates from telomere regions during mitosis.

The CLEM factor was calculated to be 5 in these experiments which means 5 times reduction in phototoxicity and photobleaching. In practice, an even stronger reduction in phototoxicity and photobleaching was observed. This indicates that cells can cope with a limited level of oxidative stress but above all it shows the necessity of CLEM for successful live-cell imaging during longer periods of time.

CLEM implementation prospects

CLEM in advanced scanning microscopy

Two-photon excitation microscopy

The concept of two-photon excitation is based on the fact that two photons of low energy can sum up their energy and excite a fluorophore with the double energy when they arrive in a spot in the object at the same timepoint [19]. However, the probability of simultaneous absorption of two photons is extremely low. Therefore, a high flux of excitation photons is required and thus usually a femtosecond laser is applied for two-photon excitation microscopy. Because two photons are needed to be absorbed to excite a fluorophore, the probability for fluorescent emission from the fluorophores increases quadratically with the excitation intensity. Consequently, there is no need for a pinhole to reject out-of-focus fluorescence as with a standard single-photon (confocal) excitation microscope.

Photons of low energy (i.e. longer wavelength) are scattered to a lesser degree than photons with a shorter wavelength and due to the absence of a pinhole in two-photo microscopy even scattered photons are detected. These phenomena enable deeper penetration into tissue and deeper imaging in tissue. In very thin objects such as isolated cells, single-photon (confocal) microscopes

can produce images with higher optical resolution because of the shorter excitation wavelength. Although lower-energy photons are less likely to cause damage, there is a high flux of excitation photons required. It is often claimed that phototoxicity and photobleaching induced by two-photo microscopy is less than that induced by single-photon confocal microscopy[19;20]. However, this is not always the case [21-25]. Total exposure required for equivalent fluorescence generation is at least an order of magnitude higher in two-photon microscopy then in single-photon microscopy [21]. Excitation intensity has to be kept low, because nonlinear photodamage sets in when laser power is increased above a certain threshold [22]. This all can lead to phototoxicity, photobleaching and photothermal effects (heating) especially in the focal volume hampering fluorescence live-cell and in-vivo imaging.

The technique of implementing CLEM technology in two-photon excitation microscopy is similar to the implementation in standard scanning confocal microscopy. The reduction of illumination in the background and the bright foreground reduces phototoxicity, photobleaching and photo-thermal effects in the focal volume. Because excitation of fluorophores in two-photon excitation microscopy only takes place in the focal volume, the reduction of illumination in the background has less effect as compared with single-photon (confocal) microscopy where excitation of fluorophores in out-of-focus objects is reduced as well. Two-photon excitation microscopy is expected to benefit considerably from the implementation of CLEM when performing live-cell and live-tissue imaging.

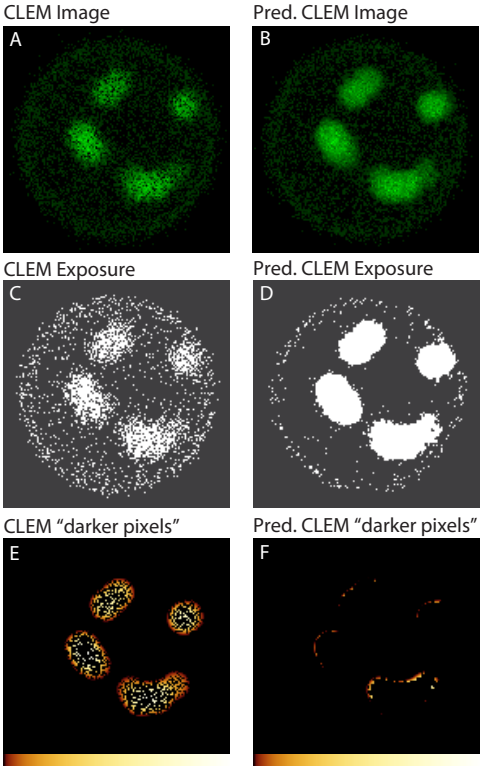

Figure 3 Computer simulation of reduction of illumination in the background in CLEM and predictive CLEM (pred. CLEM) with S/N=6 showing generation of artifacts in the image. These artifacts are visible as erratic "darker pixels" in the foreground. In CLEM, photons that are collected in each single pixel are used for the feedback regulation of light exposure. In predictive CLEM, information of already measured neighbouring pixels is used to estimate light exposure for an upcoming pixel. The CLEM image and the predictive CLEM image are shown in **A** and **B,** respectively**.** The light exposure represented as an image is shown for CLEM and predictive CLEM in **C** and **D,** respectively. The erratic "darker pixels" caused by reduction of illumination as if the weak foreground was background were detected by a special adaptive filter in CLEM and predictive CLEM and shown in **E** and **F,** respectively. The deviation of the detected "darker pixel" from its correct value is represented on the basis of the colorscale at the bottom of **E** and **F**.

4Pi confocal microscopy

The principle of a 4Pi confocal microscope is the use of two opposing lenses to generate images with increased resolution in depth

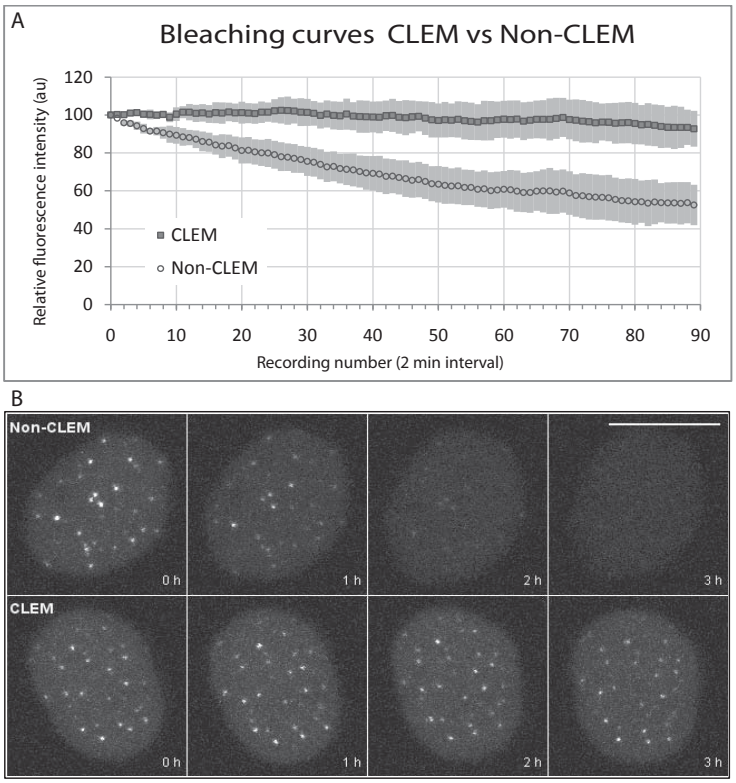

Figure 4 A series of similar-sized nuclei of ECV-304 cells stably expressing TRF2-mCitrine are imaged for 3 hours at 2 min interval under CLEM conditions and another under non-CLEM conditions. (**A**) Bleaching curves illustrate the superior conditions of CLEM (dark squares) versus non-CLEM (light circles). The data points represent averages of 6 nuclei and the standard deviations are represented by grey bars. The images below the graph demonstrate the preservation of image quality and telomere resolvability under CLEM conditions throughout the imaging period, whereas non-CLEM illumination causes rapid bleaching and reduction of image quality. Scale bar: 10 µm. This figure is reproduced from Cytometry Ref. 18 © (2009) Wiley InterScience inc.

by coherent superposition of excitation and emission light [26]. A typical axial resolution of a 4Pi confocal microscope is approx. 2 times better (100 nm) than a standard confocal microscope. The benefits of the implementation of CLEM are exactly the same as in a standard confocal microscope.

Stimulated emission depletion (STED) microscopy

The resolution of a standard confocal scanning microscope is limited to the focused spot size of the excitation light (i.e. focal volume). This size is approximately the wavelength of excitation light. STED microscopy reduces the size of the excited region by using a very short excitation pulse which is immediately followed by a "depletion" pulse that is tuned to the emission wavelength of the fluorophore [27]. This depletion pulse forces electrons from the excited state to a lower energy state by stimulated emission. The wavefront of the depletion beam is focused into a ring with a dark spot of zero intensity in the center. Using a bright depletion pulse causes almost all electrons to be excited by the excitation pulse to return to the ground state. This leaves only the region of the sample close to the axis of the depletion beam excited. The remaining fluorescence is detected by the microscope. STED improves lateral resolution up to 12-fold over standard confocal scanning microscopy. Axial resolution can be improved by combining STED with 4Pi microscopy [27].

Phototoxicity and photobleaching in STED

microscopy is a major problem and has been found to be strongly nonlinear depended on the power and duration of the STED depletion pulse [28-31]. Therefore, STED can benefit greatly by implementing CLEM. Implementation of CLEM in STED microscopy can be done in the same way as in a standard confocal microscope with the exception that both the excitation and depletion illumination have to be controlled.

CLEM in multi-point scanning microscopy

A major drawback of (single-point) scanning microscopes is the relatively low acquisition speed. A way to overcome this problem is to use multi-point scanning microscopes. Phototoxicity and photobleaching is lower as compared with single-point scanning confocal microscopy [32;33]. First, the higher sensitivity of CCD cameras that are typically used as a detector in multi-point scanning microscopes enable reduction of phototoxicity and photobleaching. The quantum efficiency of CCD cameras (up to 90%) is higher than that of PMTs (maximum 30%). Second, in single-point scanning, a high intensity laser beam passes the sample and illuminates every region intensely, but only for a short period of time (2–10 µs). As a result, the excitation light has to be intense in order to excite enough fluorophores during this short time and produces high amounts of free radicals in a short time in a particular spot in cells. In multi-point scanning, the excitation light is split into many beams and has correspondingly lower intensity in spots. However, several of these beams pass over the same region sequentially and the emission of all their passes is collected during the camera exposure time. The illumination time per pixel is therefore significantly (1000-fold) longer. Consequently, phototoxicity and photobleaching is reduced because a low amount of free radicals is produced in one particular spot in cells at each time. Two of the most commonly implementations of multi-point microscopes are the spinning-disk microscope and the programmable array microscope (PAM).

Spinning disk confocal microscope

A spinning disk confocal microscope consists of a rotating disk with multiple pinholes and a CCD camera[4;32]. The pinholes on the disk are arranged in a pattern that allows every location of an image to be covered when the disk is rotated. A homogeneous field of excitation light illuminates a section of the spinning disk. The light going through the pinholes forms a set of beams corresponding to the pinhole pattern and sweeps the field of view because of the disk rotation. Every beam in itself is confocal with the same pinhole serving for the excitation as well as emission.

Implementation of CLEM in spinning disk confocal microscopy is complicated. The various beams generated by the spinning disk scan pixels randomly and thus it is great challenge to control light exposure per pixel. Addition of an extra spatial light modulator synchronized with the spinning disk and the CCD camera to control light exposure is possible, but needlessly complicates the microscope.

Programmable array microscope (PAM)

A PAM incorporates a spatial light modulator (SLM) placed in the image plane of a wide-

field fluorescence microscope, where it is used to generate arbitrary patterns of conjugate illumination and detection elements [34;35]. The SLM dissects the fluorescent light imaged into a focal conjugate image formed by in-focus emission light, and a non-conjugate image formed by out-of-focus emission light. There are two different schemes for confocal imaging using PAM. In the first scheme, a grid of points is shifted to scan the complete object (as with the spinning-disk confocal microscope). The second, faster approach, uses a short tiled pseudorandom sequence of two-dimensional patterns. In the first case, the conjugate image is equivalent to a confocal image and the non-conjugate image is equivalent to a conventional wide-field image minus the confocal image. In the second case, the conjugate image and the non-conjugate image are the sum and the difference, respectively, of a conventional wide-field and a confocal image. Consequently, the pseudorandom sequence approach requires post-processing to retrieve the confocal part.

CLEM has been implemented in a PAM by superimposing an illumination mask on the arbitrary scanning patterns used for confocal microscopy [36;37]. In PAM-CLEM, acquisition is broken up in several successive intermediate images that are later summed to one image. CLEM uses the first intermediate image to determine which part is background and which part is foreground and adjust the illumination mask accordingly. When performing PAM-CLEM live-cell imaging previously acquired images in time can be used as well. Here, PAM-CLEM is a combination of CLEM using the value in single pixels and predictive CLEM. Predictive CLEM cannot be applied in single image PAM-CLEM because pixels are read out after the acquisition of one complete image.

Reconstruction of the CLEM-image from the masked illumination and the detected image is not as simple as the linear extrapolation used in the single-point scanning confocal microscope. The CLEM illumination mask superimposed on the scanning pattern, is imaged onto the sample. Consequently, the illumination mask is blurred by the excitation point spread function (PSF) of the microscope. At the same time, the image detected by the CCD camera of the fluorescent sample is also blurred by the emission PSF. Reconstruction of the CLEM image by simple extrapolation using the mask and the detected image results in considerable artifacts visible at the border of objects (Fig. 5A). Reconstruction of the image by extrapolation can also be performed with the use of the blurred mask and the fluorophore distribution of the object. Blurring the mask is carried out by a convolution with the excitation PSF, but the fluorophore distribution in the object can only be estimated by deconvolution [38-40]. However, in the reconstructed CLEM image border effects are still noticeable (data not shown). A more conservative approach is to expand the illumination mask beyond the borders. The original mask provided by CLEM is used for the reconstruction, but for illumination the mask is dilated by a number of pixels. In this way, the border effects can be avoided (Fig. 5B). The number of dilations necessary depends on the shape of the point spread function. Obviously, expanding the border reduces the CLEM effect. It has been shown that PAM-CLEM with this approach leads to

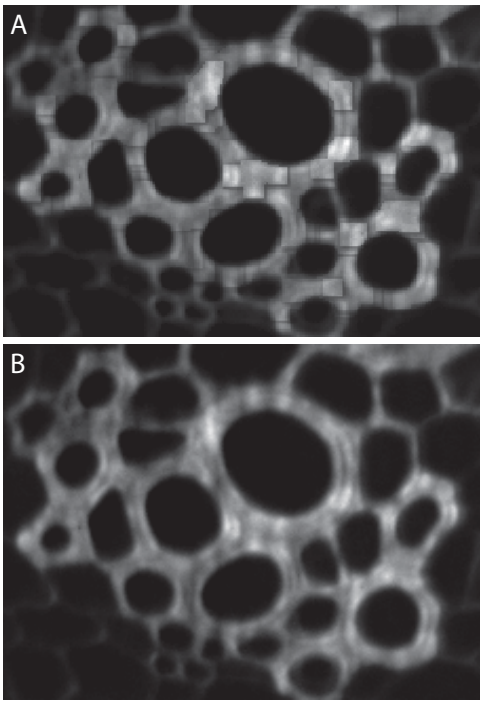

Figure 5 Avoidance of border effects in PAM-CLEM by expanding the border of the illumination mask. A dicot root sample is acquired using 10 successive intermediate images that are summed to one image. The CLEM illumination mask is created by using the first intermediate image to determine which part is background and which part is foreground. (**A**) The reconstruction of the CLEM image by extrapolation shows border effects and consequently deteriorates image quality considerably. (**B**) These border effects are avoided when the illumination mask is expanded by dilation but for the CLEM reconstruction the original mask is used. Images courtesy of Wouter Caarls Ref. 62.

a more than 2-fold decrease in the rate of photobleaching [36;37]. Further study on how to design, superimpose and apply the illumination mask and how to reconstruct the CLEM-image in CLEM-PAM is necessary to reduce image artefacts in the form of border effects and thus optimize image quality.

CLEM in wide-field microscopy

Conventional wide-field microscopy combined with deconvolution

In conventional fluorescence wide-field microscopy, light emitted from the entire depth of the excited sample is collected by a sensitive CCD camera. Consequently, wide-field microscopy is very efficient in collecting emission light and very fast because an image of the entire field of view is acquired at once. A 3D image can be obtained by acquiring a through focus stack combined with image deconvolution afterwards to reduce out-of-focus-light and improve contrast and resolution [38-40]. Fluorescence wide-field live-cell deconvolution microscopy (FWDM) has been used with great success [13;41-45]. Currently, FWDM induces the smallest amount of phototoxicity and photobleaching in living cells of all fluorescence live-cell microscopy techniques. Therefore, implementation of CLEM in FWDM would make it the most efficient fluorescence live-cell microscope at this moment in time. To control light exposure in FWDM, a SLM is placed in front of the illuminator of a wide-field microscope and imaged onto the specimen. However, the illumination mask is blurred by the excitation PSF and the image detected by the CCD of the fluorescent sample is blurred by the emission PSF of the microscope. Consequently, a reconstructed CLEM image in FWDM-CLEM has a border effect that is even more pronounced than in PAM-CLEM because out-of-focus light reaches the CCD camera as well. Expansion of the illumination mask beyond the borders (as in PAM-CLEM) helps to reduce this effect but does not completely eliminate it. A live-cell experiment with H2B-GFP-labeled HeLa Cells in FWDM-CLEM shows a 3.5-fold reduction in

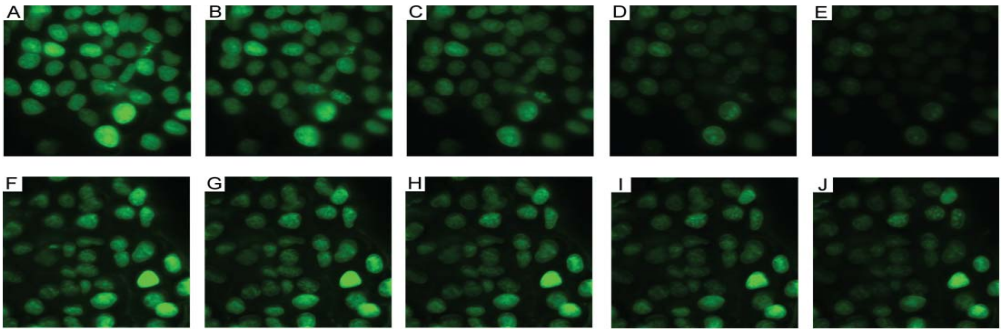

Figure 6 Bleaching of H2B-GFP-labelled HeLa cells in wide-field fluorescence microscopy under non-CLEM (**A-E**) and CLEM (**F-J**) conditions. After illumination of 85 stacks of 20 z-slices each (500 nm/slice), the non-CLEM fluorescence intensity in the center-slice is reduced to 10% (**E**) whereas CLEM fluorescence intensity was reduced to 50% (**J**) of the original fluorescence intensity. Comparison of non-CLEM with CLEM at 50% of the original fluorescence shows a 3.5-fold reduction of the bleach rate under CLEM conditions.

photobleaching [46] (Fig. 6). Again, problems such as the design and application of the illumination mask and the reconstruction of the CLEM image in FWDM-CLEM have to be addressed to reduce image artefacts and thus optimize image quality like in PAM-CLEM.

Structured illumination microscopy

Structured illumination in wide-field microscopy combines optical and computational methods that remove out-of-focus information from an image [47]. This method allows for optical sectioning, improved axial resolution (i.e. z-axis resolution), and improved lateral resolution due to the removal of out-of-focus light when compared to standard wide-field microscopy. Recently, a new structured illumination wide-field microscopy was described, which produces 100-nm-scale spatial resolution in all three dimensions by using a microscope that has two opposing objective lenses (4Pi) [48]. Structured illumination has been used successfully in living-cell microscopy [49;50]. Implementation of CLEM in structured illumination microcopy seems to be very difficult. Superimposing the illumination mask on the structured illumination makes reconstruction of the image extremely complicated.

Photo-activated localization microscopy (PALM , STORM)

Photo-activated localization microscopy achieves high lateral resolution (<50 nm) by precisely localizing individual photo-activatable fluorophores [51-56]. However, this approach requires large numbers of raw images (typically more then 1000) and is therefore limited in speed. Recently, a form of PALM decreased the acquisition time for a single image from hours to around 25-60 sec by locating a subset of available molecules per frame [57]. This approach decreases the lateral resolution to approx. 60 nm but allows live-cell imaging. Photobleaching is in most photo-activated localization microscopy techniques part of the imaging process but phototoxicity is a major problem. For these reasons, photon-tolerant cell lines are selected [57].

Implementation of CLEM in PALM is possi-

ble by controlling the photo-activation light with a SLM. In this way, only fluorophores needed to improve image quality are activated. The activation mask can be determined from already acquired intermediate images and also previous images in time.

Light sheet-based microscopy (SPIM)

Light sheet-based microscopy (SPIM) is a method for imaging large fluorescent samples [58]. To achieve optical sectioning, the sample is illuminated with a sheet of light. The fluorescence is imaged with a standard wide-field microscope equipped with a CCD camera. Only the plane that is in focus is illuminated, thus limiting phototoxicity and photobleaching. The sample is embedded in a cylinder of agarose gel suitable for living specimens. SPIM can acquire 3D images in large living samples with a axial resolution exceeding that of a fluorescence confocal microscope by using a reconstruction algorithm that performs a joint deconvolution of data acquired along multiple directions [59].

Implementation of CLEM in SPIM is possible to some extent. Spatial control of light exposure is hampered by the sheet illumination and reconstruction of the images is complicated by possible non-homogeneous bleaching of the fluorophores in the sample.

Total internal reflection fluorescence microscopy (TIRFM)

Live-cell TIRFM uses an evanescent wave to selectively illuminate fluorophores in a restricted region of the cells immediately adjacent to the glass-'sample medium' interface [60]. TIRFM uses a standard wide-field microscope equipped with a CCD camera. An evanescent wave is generated only when the incident light is totally reflected at the glass-'sample medium' interface and penetrates to a depth of approximately 100 nm into the sample medium thus limiting phototoxicity and photobleaching in the imaged cells [61].

The total internal reflection technique used to generate the evanescent in TIRFM wave makes implementation of CLEM unfeasible.

Conclusion

CLEM technology can be used in various fluorescence live-cell microscope techniques, but the benefits of CLEM implementation vary (Table 1). For different reasons, implementation of CLEM in spinning disk, light-sheet based, TIRFM, and to a lesser extent structured illumination microscopy is complicated. Implementation of CLEM in conventional wide-field microscopy seems possible but also difficult because of the lack of true optical sectioning. For this reason, border effects occur in the reconstructed CLEM image. These border effects also occur in PAM-CLEM but can be avoided by expanding the illumination mask. In contrast, CLEM implementation in single point scanning microscopes is relatively simple, because spatial control of the light dose and reconstruction of the CLEM image is easy. Hence, implementation of CLEM is straightforward in two-photon, 4Pi and STED microscopy where live-cell imaging will benefit substantially from strong reduction in phototoxicity and photobleaching provided by CLEM.

Table 1 CLEM in live-cell microscopy, implementation prospects

	Live-cell imaging	Nm resolution (lateral, axial)	Acquisition speed	Detection efficiency	Photo-damage	CLEM implementation
Standard confocal microscopy	+	++ (150, 400)	- Point-scanning	- - PMT 30%	- - -	++++
Two-photon microscopy	+ / - Depends on laser power	+ (300, 800)	- Point-scanning	- PMT no pinhole	- - / - - - -	++++
4PI microscopy	+	+++ (150, 100)	- Point-scanning	- PMT no pinhole	- -	++++
Stimulated emission depletion (STED) microscopy	+ Small volume	+++ (<50, 400)	- Point-scanning	- PMT no pinhole	- - - - High power	++++
STED 4PI microscopy	+ Small volume	++++ (50, 100)	- Point-scanning	- PMT no pinhole	- - - High power	++++
Spinning disk microscopy	++	++ (150, 400) Thin sample	+ Multi-point scanning	++ CCD Up to 90%	- Low power	-
Programmable array (PAM) microscopy	++	++ (150, 400) Thin sample	+ Multi-point scanning	++ CCD	- Low power	+++ Expanded mask
Wide-field microscopy & deconvolution	+++ Fast	+ (200, 500)	++ Entire field of view	+++ CCD no pinhole	++ Low power	++ Expanded mask, image artefacts
Structured illumination microscopy	+(2D) - (3D)	++ (100, 400 2D) (100, 100 3D)	+ 2D 5 images 3D 15 images	+++ CCD no pinhole	+ Multiple images	+/- Reconstruction difficult
Photo-act. loc. microscopy (PALM, STORM)	- - Very slow	+++ (50, 400)	- - - > 1000 images	+++ CCD no pinhole	+ Multiple images	++
Light-sheet microscopy (SPIM)	+ Slow	+ (400, 400)	- - Multiple images	+++ CCD no pinhole	+ Multiple images	- Mask and reconstruction difficult
Total internal reflection microscopy (TIRFM)	+++	++ (200, 100)	++ Entire field of view	+++ CCD no pinhole	+++ 100 nm depth	- -

Reference list

(1) Hoebe, R. A.; Van Oven, C. H.; Gadella, T. W., Jr.; Dhonukshe, P. B.; Van Noorden, C. J.; Manders, E. M. Controlled Light-Exposure Microscopy Reduces Photobleaching and Phototoxicity in Fluorescence Live-Cell Imaging. *Nat. Biotechnol.* **2007,** *25,* 249-253.

(2) Manders, E. M. M. Method and apparatus for shaping an image of an object. WO2004102249. *Patent*, **2004**.

(3) Hoebe, R.A.; Manders, E.M.M. Method for imaging an object. PCT/NL2009/0505182. *Patent Pending*, **2009**.

(4) Stephens, D. J.; Allan, V. J. Light Microscopy Techniques for Live Cell Imaging. *Science* **2003,** *300,* 82-86.

(5) Frigault, M. M.; Lacoste, J.; Swift, J. L.; Brown, C. M. Live-Cell Microscopy - Tips and Tools. *J Cell Sci* **2009,** *122,* 753-767.

(6) Dixit, R.; Cyr, R. Cell Damage and Reactive Oxygen Species Production Induced by Fluorescence Microscopy: Effect on Mitosis and Guidelines for Non-Invasive Fluorescence Microscopy. *Plant J.* **2003,** *36,* 280-290.

(7) Dobrucki, J. W.; Feret, D.; Noatynska, A. Scattering of Exciting Light by Live Cells in Fluorescence Confocal Imaging: Phototoxic Effects and Relevance for FRAP Studies. *Biophysical Journal* **2007,** *93,*

1778-1786.

(8) Eggeling, C.; Widengren, J.; Rigler, R.; Seidel, C. A. M. Photobleaching of Fluorescent Dyes Under Conditions Used for Single-Molecule Detection: Evidence of Two-Step Photolysis. *Analytical Chemistry* **1998,** *70,* 2651-2659.

(9) Lippincott-Schwartz, J.; Altan-Bonnet, N.; Patterson, G. H. Photobleaching and Photoactivation: Following Protein Dynamics in Living Cells. *Nat. Cell Biol.* **2003,** *Suppl,* S7-14.

(10) Song, L.; Varma, C. A.; Verhoeven, J. W.; Tanke, H. J. Influence of the Triplet Excited State on the Photobleaching Kinetics of Fluorescein in Microscopy. *Biophys. J.* **1996,** *70,* 2959-2968.

(11) Knight, M. M.; Roberts, S. R.; Lee, D. A.; Bader, D. L. Live Cell Imaging Using Confocal Microscopy Induces Intracellular Calcium Transients and Cell Death. *Am J Physiol Cell Physiol* **2003,** *284,* C1083-C1089.

(12) Centonze, V.; Pawley, J. B. Tutorial on Practical Confocal Microscopy and Use of the Confocal Test Specimen. In *Handbook of Biological Confocal Microscopy*; Pawley, J. B., Ed.; Plenum Press: New York, **1995**.

(13) Pawley, J. B.; Masters, B. R. Handbook of Biological Confocal Microscopy, Third Edition. *Journal of Biomedical Optics* **2008,** *13,* 029902-029903.

(14) Sheppard, C. J. R.; Gan, X.; Gu, M.; Roy, M. Signal-to-Noise in Confocal Microscopes. In *Handbook of Biological Confocal Microscopy*; Pawley, J. B., Ed.; Plenum Press: New York, **1995**.

(15) Brakenhoff, G. J.; van der Voort, H. T.; van Spronsen, E. A.; Nanninga, N. Three-Dimensional Imaging by Confocal Scanning Fluorescence Microscopy. *Ann. N. Y. Acad. Sci.* **1986,** *483,* 405-415.

(16) Hoebe, R. A.; van der Voort, H. T.; Stap, J.; Van Noorden, C. J.; Manders, E. M. Quantitative Determination of the Reduction of Phototoxicity and Photobleaching by Controlled Light Exposure Microscopy. *J. Microsc.* **2008,** *231,* 9-20.

(17) Hoebe, R. A.; Van Noorden, C. J.; Manders, E. M. Noise effects and filtering in controlled light exposure microscopy (CLEM), *Submitted*. **2009**.

(18) De Vos, W. H.; Hoebe, R. A.; Joss, G. H.; Haffmans, W.; Baatout, S.; van Oostveldt, P.; Manders, E. M. Controlled Light Exposure Microscopy Reveals Dynamic Telomere Microterritories Throughout the Cell Cycle. *Cytometry A* **2008**.

(19) Denk, W.; Strickler, J. H.; Webb, W. W. Two-Photon Laser Scanning Fluorescence Microscopy. *Science* **1990,** *248,* 73-76.

(20) Diaspro, A.; Robello, M. Two-Photon Excitation of Fluorescence for Three-Dimensional Optical Imaging of Biological Structures. *J. Photochem. Photobiol. B* **2000,** *55,* 1-8.

(21) Brakenhoff, G. J.; Muller, M.; Ghauharali, R. I. Analysis of Efficiency of Two-Photon Versus Single-Photon Absorption of Fluorescence Generation in Biological Objects. *J. Microsc.* **1996,** *183,* 140-144.

(22) De, A. K.; Goswami, D. Exploring the Nature of Photo-Damage in Two-Photon Excitation by Fluorescence Intensity Modulation. *Journal of Fluorescence* **2009,** *19,* 381-386.

(23) Hopt, A.; Neher, E. Highly Nonlinear Photodamage in Two-Photon Fluorescence Microscopy. *Biophys. J.* **2001,** *80,* 2029-2036.

(24) Eggeling, C.; Volkmer, A.; Seidel, C. A. M. Molecular Photobleaching Kinetics of Rhodamine 6G by One- and Two-Photon Induced Confocal Fluorescence Microscopy. *Chemphyschem* **2005,** *6,* 791-804.

(25) Patterson, G. H.; Piston, D. W. Photobleaching in Two-Photon Excitation Microscopy. *Biophys. J.* **2000,** *78,* 2159-2162.

(26) Hell, S.; Stelzer, E. H. K. Properties of A 4Pi Confocal Fluorescence Microscope. *Journal of the Optical Society of America A-Optics Image Science and Vision* **1992,** *9,* 2159-2166.

(27) Hell, S. W.; Wichmann, J. Breaking the Diffraction Resolution Limit by Stimulated-Emission - Stimulated-Emission-Depletion Fluorescence Microscopy. *Optics Letters* **1994,** *19,* 780-782.

(28) Dyba, M.; Hell, S. W. Photostability of a Fluorescent Marker Under Pulsed Excited-State Depletion Through Stimulated Emission. *Applied Optics* **2003,** *42,* 5123-5129.

(29) Eggeling, C.; Kastrup, L.; Blom, H.; Hell, S. W. Enhancing the Applicability of Fluorescence Fluctuation Spectroscopy Through Reduced Focal Volumes Generated by Stimulated Emission Depletion. *Biophysical Journal* **2005,** *88,* 662A.

(30) Hell, S. W. Toward Fluorescence Nanoscopy. *Nature Biotechnology* **2003,** *21,* 1347-1355.

(31) Hell, S. W.; Dyba, M.; Jakobs, S. Concepts for Nanoscale Resolution in Fluorescence Microscopy. *Current Opinion in Neurobiology* **2004,** *14,* 599-609.

(32) Gräf, R.; Rietdorf, J.; Zimmermann, T. Live Cell Spinning Disk Microscopy. 2005.

(33) Wang, E.; Babbey, C. M.; Dunn, K. W. Performance Comparison Between the High-Speed Yokogawa Spinning Disc Confocal System and Single-Point Scanning Confocal Systems. *J Microsc.* **2005,** *218,* 148-159.

(34) Heintzmann, R.; Hanley, Q. S.; Arndt-Jovin, D.; Jovin, T. M. A Dual Path Programmable Array Microscope (PAM): Simultaneous Acquisition of Conjugate and Non-Conjugate Images. *J Microsc.* **2001,** *204,* 119-135.

(35) Hanley, Q. S.; Verveer, P. J.; Gemkow, M. J.; Arndt-Jovin, D.; Jovin, T. M. An Optical Sectioning Programmable Array Microscope Implemented With a Digital Micromirror Device. *J Microsc.* **1999,** *196,* 317-331.

(36) Caarls, W.; de Vries, A. H. B.; Arndt-Jovin, D.; Jovin, T. M. Controlled Light Exposure Microscopy with the Programmable Array Microscope *(in prepara-*

tion). **2009**.

(37) Caarls, W.; de Vries, A. H. B.; Arndt-Jovin, D.; Jovin, T. M. Arbitrary and Dynamic Patterning in a Programmable Array Microscope. *Focus on Microscopy, Congress*. **2009**. Krakow, Poland.

(38) Clendenon, J. L.; Byars, J. M.; Hyink, D. P. Image Processing Software for 3D Light Microscopy. *Nephron Experimental Nephrology* **2006,** *103,* E50-E54.

(39) McNally, J. G.; Karpova, T.; Cooper, J.; Conchello, J. A. Three-Dimensional Imaging by Deconvolution Microscopy. *Methods-A Companion to Methods in Enzymology* **1999,** *19,* 373-385.

(40) van der Voort, H. T. M.; Strasters, K. C. Restoration of Confocal Images for Quantitative Image-Analysis. *Journal of Microscopy-Oxford* **1995,** *178,* 165-181.

(41) Gasser, S. M. Visualizing Chromatin Dynamics in Interphase Nuclei. *Science* **2002,** *296,* 1412-1416.

(42) Helmke, B. P.; Goldman, R. D.; Davies, P. F. Rapid Displacement of Vimentin Intermediate Filaments in Living Endothelial Cells Exposed to Flow. *Circ Res* **2000,** *86,* 745-752.

(43) Swedlow, J. R.; Platani, M. Live Cell Imaging Using Wide-Field Microscopy and Deconvolution. *Cell Structure and Function* **2002,** *27,* 335-341.

(44) Waterman-Storer, C. M. Microtubules and Microscopes: How the Development of Light Microscopic Imaging Technologies Has Contributed to Discoveries About Microtubule Dynamics in Living Cells. *Molecular Biology of the Cell* **1998,** *9,* 3263-3271.

(45) Krawczyk, P. M.; Stap, J.; Hoebe, R. A.; Van Oven, C. H.; Kanaar, R.; Aten, J. A. Analysis of the Mobility of DNA Double-Strand Break-Containing Chromosome Domains in Living Mammalian Cells. *Methods Mol. Biol.* **2008,** *463,* 309-320.

(46) Zoon, P. D.; Lambrechts, S. A. G.; Hoebe, R. A.; Manders, E. M. M. Controlled light exposure microscopy - The widefield implementation *(in preparation)*. **2009**.

(47) Neil, M. A. A.; Wilson, T.; Juskaitis, R. A Light Efficient Optically Sectioning Microscope. *Journal of Microscopy-Oxford* **1998,** *189,* 114-117.

(48) Shao, L.; Isaac, B.; Uzawa, S.; Agard, D.; Sedat, J.; Gustafsson, M. I5S: Wide-Field Light Microscopy With 100-Nm-Scale Resolution in Three Dimensions. *Biophys J* **2008,** *94,* 4971-4983.

(49) Hirvonen, L. M.; Wicker, K.; Mandula, O.; Heintzmann, R. Structured Illumination Microscopy of a Living Cell. *European Biophysics Journal with Biophysics Letters* **2009,** *38,* 807-812.

(50) Kner, P.; Chhun, B. B.; Griffis, E. R.; Winoto, L.; Gustafsson, M. G. L. Super-Resolution Video Microscopy of Live Cells by Structured Illumination. *Nature Methods* **2009,** *6,* 339-U36.

(51) Betzig, E.; Patterson, G. H.; Sougrat, R.; Lindwasser, O. W.; Olenych, S.; Bonifacino, J. S.; Davidson, M. W.; Lippincott-Schwartz, J.; Hess, H. F. Imaging Intracellular Fluorescent Proteins at Nanometer Resolution. *Science* **2006,** *313,* 1642-1645.

(52) Geisler, C.; Schonle, A.; Von Middendorff, C.; Bock, H.; Eggeling, C.; Egner, A.; Hell, S. W. Resolution of Lambda/10 in Fluorescence Microscopy Using Fast Single Molecule Photo-Switching. *Applied Physics A-Materials Science & Processing* **2007,** *88,* 223-226.

(53) Hess, S. T.; Girirajan, T. P. K.; Mason, M. D. Ultra-High Resolution Imaging by Fluorescence Photoactivation Localization Microscopy. *Biophysical Journal* **2006,** *91,* 4258-4272.

(54) Lemmer, P.; Gunkel, M.; Baddeley, D.; Kaufmann, R.; Urich, A.; Weiland, Y.; Reymann, J.; Muller, P.; Hausmann, M.; Cremer, C. SPDM: Light Microscopy With Single-Molecule Resolution at the Nanoscale. *Applied Physics B-Lasers and Optics* **2008,** *93,* 1-12.

(55) Lidke, K. A.; Rieger, B.; Jovin, T. M.; Heintzmann, R. Superresolution by Localization of Quantum Dots Using Blinking Statistics. *Optics Express* **2005,** *13,* 7052-7062.

(56) Rust, M. J.; Bates, M.; Zhuang, X. W. Sub-Diffraction-Limit Imaging by Stochastic Optical Reconstruction Microscopy (STORM). *Nature Methods* **2006,** *3,* 793-795.

(57) Shroff, H.; Galbraith, C. G.; Galbraith, J. A.; Betzig, E. Live-Cell Photoactivated Localization Microscopy of Nanoscale Adhesion Dynamics. *Nature Methods* **2008,** *5,* 417-423.

(58) Huisken, J.; Swoger, J.; Del Bene, F.; Wittbrodt, J.; Stelzer, E. H. K. Optical Sectioning Deep Inside Live Embryos by Selective Plane Illumination Microscopy. *Science* **2004,** *305,* 1007-1009.

(59) Verveer, P. J.; Swoger, J.; Pampaloni, F.; Greger, K.; Marcello, M.; Stelzer, E. H. K. High-Resolution Three-Dimensional Imaging of Large Specimens With Light Sheet-Based Microscopy. *Nature Methods* **2007,** *4,* 311-313.

(60) Axelrod, D. Cell-Substrate Contacts Illuminated by Total Internal Reflection Fluorescence. *The Journal of Cell Biology* /4**, 1989***,* 141-145.

(61) Borejdo, J.; Muthu, P.; Talent, J.; Gryczynski, Z.; Calander, N.; Akopova, I.; Shtoyko, T.; Gryczynski, I. Reduction of Photobleaching and Photodamage in Single Molecule Detection: Observing Single Actin Monomer in Skeletal Myofibrils. *Journal of Biomedical Optics* **2008,** *13,* 034021-10.

(62) Caarls, W. Personal Communication. **2009**.